High temperature annealing of micrometric Zn_2SiO_4:Mn phosphor powders in fluidized bed

Shila Alavi[a], Jeannette Dexpert-Ghys[b] and Brigitte Caussat[a,*]

[a]Laboratoire de Génie Chimique, UMR CNRS 5503, ENSIACET/INPT,
5 rue Paulin Talabot, BP 1301, 31106 Toulouse Cedex 1, France
[b]CEMES, UPR CNRS 8011, 29 rue Jeanne Marvig, 31055 Toulouse Cedex 4, France

Contact : Brigitte.Caussat@ensiacet.fr

Abstract

Micrometric $Zn_{1.8}Mn_{0.2}SiO_4$ phosphor powders prepared by spray pyrolysis have been annealed between 900 and 1200°C under ambient air atmosphere to exalt their luminescence properties. Two original gas-solid fluidization processes have been tested in order to limit sintering phenomena, and the post-treated products have been compared with those annealed using a conventional process in crucible. The crystallinity, the size distribution, the outer morphology and the luminescence properties of powders before and after treatment have been analysed. Massive sintering phenomena occur in crucible from 1000°C, whereas the original granulometry and spherical morphology are preserved till 1100°C in fluidized bed. The luminescence efficiencies are comparable for the three processes and maximal after annealing at 1200°C. It has been established that residual ZnO and manganese ions at oxidation state higher than 2, still present after treatment at 1100°C, are detrimental to good luminescence efficiency. Both disappear from samples post-treated at 1200°C.

Keywords: A. Inorganic compounds; B. Crystal growth, C. X Ray diffraction, C. Electron microscopy, D. Luminescence

1. Introduction

The manganese doped willemite powder $Zn_{2-x}Mn_xSiO_4$ is an efficient green phosphor widely used in fluorescent lamps or emissive displays. It exhibits a good efficiency under VUV (vacuum ultra violet) excitation, and is in consequence employed for plasma display panels (PDPs) [1-3]. Many researches have been carried out to improve the photo luminescence properties of $Zn_2SiO_4:Mn^{2+}$, especially by changing the doping molar level [Mn]/([Zn]+[Mn]). For PDPs applications, the doping level must be high enough to reduce the emitting lifetime without loosing too much efficiency [4,5]. The synthesis process has also much effect on the properties of the phosphor, i.e. chemical resistance, handling facility, and luminescent efficiency.

The powders are conventionally synthesized by solid-state reactions, requiring repeated high temperature treatments (1400 °C for several hours) and millings to homogenize the powder and reduce the average particle size. These processes provide powders with large size distributions and irregular shapes. This is the reason why alternative synthesis routes are under scope to control the particles morphology. Fine particles (about 1μm in average size), with a regular shape - preferably spherical - have been recommended to ensure higher packing densities on flat panels, which means less matter needed.

Spray-pyrolysis (SP) is a particularly attractive route of synthesis: it is well known to generate micrometric powders with spherical shape and may be employed for the synthesis of multicomponent materials. Moreover this process possibly works at a large scale. The SP synthesis of the green phosphor has been reported by several groups [6-9].

In order to get good luminescence properties, post-synthesis annealing of SP powders is absolutely necessary. This post heat treatment is classically carried out in a static mode, either in a crucible of a few grams of particles at the lab scale or in moving belt furnaces at the industrial scale. The extreme temperatures required (typically 900 – 1200°C), associated with a static mode treatment often lead to sintering of particles, which means loosing the particles characteristics (i. e. spherical shape and micrometric size). Ideally the phosphor powders would be made of dense but non aggregated micrometric spheres. The post treatment is then supposed to enhance intra-particulate sintering to grow the crystalline domains, but at the same time to prevent inter-particulate sintering to keep the initial shape and size.

In this context, gas-solid fluidization appears as an interesting alternative process for crystallization of micrometric particles at such high temperatures. This technology involves intense mixing of particles by the gas flow, which limits sintering phenomena. It naturally leads to isothermal conditions, which ensures homogeneous thermal treatments. Fluidisation is easy to scale up and can reach high productivities, especially if organized in a continuous mode [10]. But the main problem is that fluidization of micrometric powders belonging to Geldart's group C of particles [11] usually leads to slugging and channeling phenomena. The inter-particle forces, especially the Van der Waals ones, are so considerable that they prevent fluidization [12]. In order to overcome the interparticle forces, fluidization can be activated by various means e.g. mechanical stirring [13], acoustic vibration [14], adding fluidizable coarse powders [15] and mechanical vibration [16].

In this work, the post heat treatment of micrometric Zn_2SiO_4:Mn powders synthesized by SP [17] was studied. Following previous results [18-19], two activated fluidization processes were tested: addition of coarse powders to fines and vibrated fluidization. In order to reveal the advantages and drawbacks of the fluidized bed (FB) processes over the conventional static method, a comparative study of the powders characteristics after heat treatment in crucible and in FB was performed. The size distribution and the morphology of the particles, the crystal structure, the degree of crystallization and the luminescence properties of the Zn_2SiO_4:Mn powders before and after thermal treatment were analysed.

2. Experimental

2.1. Setups and operating protocols

The phosphors were synthesized with a pilot-scale SP equipment using 1.6 MHz ultrasonic pellets described for instance in [17]. The micrometric droplets of the precursor solution were transported by an air flow through successively a vertical drying column, 20 cm in internal diameter and 1.8 m in length, then a horizontal decomposition/densification column, 20 cm in internal diameter and 1.8 m in length. The heating system was composed of juxtaposed electrical furnaces. Thermocouples were put on the outer wall of the reactor and allowed the temperature to be adjusted to 200°C in the drying zone and to 550°C in the decomposition zone. The solid phase was then separated from the vapour phase by a bag filter

The precursor solution employed was: $Zn(NO_3)_2$ 0.6M, $Mn(NO_3)_2$ 0.06M, SiO_2 0.31M in H_2O/CH_3OH :90/10. The nitrates were purchased from Sigma-Aldrich, whereas the silica source was the colloidal solution AS-40 from Du Pont. The resulting powder was $Zn_{1.8}Mn_{0.2}SiO_4$. With the notation most often employed in phosphors studies, it comes

$Zn_2SiO_4:Mn^{2+}$ at 10% ([Mn]/([Mn]+[Zn])) molar doping level. About 2 kg of this powder were synthesized to perform the post treatments.

A high temperature fluidized bed reactor (HTFBR) has been developed to anneal these micrometric powders. The HTFBR setup consisted first of a cylindrical alumina column, 5 cm in internal diameter and 1 m in height. A porous alumina plate provided a homogeneous gas distribution. A long wide box underneath acted as a pre-heater for the fluidizing gas. The reactor was externally heated by an electrical furnace able to operate at temperatures up to 1300°C. The experiments were performed at ambient pressure. The differential pressure drop and fluidized bed temperature were monitored continuously using a computerized data acquisition system. Dry air was used as the fluidizing gas. Its flow rate was controlled by a calibrated rotameter. A bag filter was located after the reactor exit to collect the elutriated particles.

Vibrated fluidization experiments were performed by fixing the fluidized bed column on a vibrating table. Two vibro-motors were cross-mounted on the opposite sides of the vibrating table. In order to obtain horizontal vibrations, the center of gravity of the column was adjusted to be level with the motors. The vibration amplitude was fixed by varying the eccentric weights on the vibro-motors and their frequency was controlled by an inverter. The vibration frequency could be varied from 19 to 25 Hz and the amplitude from 0.5 to 10 mm.

The experiments which involved adding large particles to fine powders were carried out in the HTFBR without exerting any external action. More details can be found elsewhere [18].

For the static mode treatment, a closed furnace of 40 × 40 × 40 cm^3 was used, made up of 4 heating elements allowing a maximum temperature of 1500°C to be reached. The sample was heated in a crucible of 6 cm in length, 2 cm in width and 1 cm in height and was placed on the bottom of the furnace under confined air atmosphere.

In all thermal treatments, the temperature was raised at a constant rate of 10°C/min. When the thermal regime was reached, the crystallisation/densification process was maintained for 30 minutes as determined from previous results [17]. The operating temperatures were fixed at 900, 1000, 1100 and 1200°C for reasons detailed in paragraph 3.1

Concerning the operating procedure, for vibrated fluidized bed experiments, a mass of 300 g of Zn_2SiO_4:Mn was introduced into the HTFBR, corresponding to an initial fixed bed height of 20 cm. When coarse powders were used as fluidization promoters, pre-mixed weights of 140 g of Zn_2SiO_4:Mn and 140 g of porous alumina were introduced into the reactor. A constant flow rate of air fluidized the bed during its heating. The fluidization ratio during annealing was always equal to 1.1. When vibrated fluidization experiments were performed, vibrations were started at the same time as the heating. In all static crystallization runs, the crucible was filled with 5 g of Zn_2SiO_4:Mn.

2.2. Characterization methods

First, the hydrodynamic behaviour of the FB activated either by vibration or by adding coarse particles was analysed by measuring the pressure drop of the gas crossing the bed, as a function of the inlet gas velocity. These measurements were performed at the four temperatures of interest, between 900 and 1200°C, at decreasing air flow rate. The results will be classically presented in terms of dimensionless pressure drop DP*, corresponding to the ratio of the measured pressure drop and of the apparent weight of the bed. When a FB is conveniently fluidized, a plateau corresponding to DP*=1 appears beyond a critical gas velocity named the minimum fluidization velocity U_{mf}. Below U_{mf}, the bed is not yet fluidized, and the pressure drop is proportional to the inlet gas velocity [10].

The powders before and after heat treatments in crucible and in activated FB were analysed as described below:

-The powder X-ray diffraction (XRD) patterns were obtained by a Seifert XRD3000 diffractometer using Cu-Kα radiation in conventional operating conditions and θ/2θ configuration to identify the crystalline phase(s). The Scherrer crystallite size was classically estimated by the Halder, Schoenig and Wanger method [20]. High temperature diffraction patterns were recorded in a Bühler HDK S1 chamber under He flux. The powder dispersed in ethanol was dropped on a Pt ribbon equipped with a thermocouple. The heating rate was 5°C.min^{-1}. Diagrams were recorded after 30 min of stabilisation at selected temperatures between 700 and 1000°C.

- Laser scattering size analyses of particles after air-dispersion were performed with a MasterSizer Malvern S setup. Each measurement corresponds to an average value calculated over 3 runs.

- The powder morphology was observed by Field Emission Gun Scanning Electron Microscopy (FEG SEM) on a JEOL 6700F.

- The luminescence excitation/emission spectra and diffuse reflectance spectra were recorded with a Hitachi F4500 spectrofluorimeter, at room temperature in the reflection mode. Powders were not crushed before measurements; they were pressed with a glass substrate on the sample holder.

3. Results and discussion

3.1. Choice of the post treatment temperatures

As illustrated in Fig. 1, the XRD pattern of the as-synthesized powder exhibits only poorly crystallized zincite ZnO; the silica is amorphous, and there is no trace of a manganese oxide. The reaction(s) leading to Zn_2SiO_4:Mn then probably occur(s) during the post treatment. Zn_2SiO_4 exhibits two crystalline phases (α and β). The so-called α-Zn_2SiO_4 (willemite) phase is the most interesting one for luminescence applications because Mn^{2+} in substitution of Zn^{2+} exhibits a bright green emission in α, whereas the emission is yellow in β [21]. The willemite is the high temperature phase. The β phase leads to the α phase by annealing at temperature higher than 900°C [22–24]. In order to choose the minimum temperature of heat treatment, the phase transformations ($2ZnO+SiO_2 \rightarrow$ β-$Zn_2SiO_4 \rightarrow$ α-Zn_2SiO_4) were studied by high temperature XRD, as shown in Fig. 1. The as-synthesized powder (by SP at 500°C) exhibited only ZnO; at 750°C were seen ZnO, β- Zn_2SiO_4 and α-Zn_2SiO_4, whereas at 900°C only the willemite α-Zn_2SiO_4.was detected.

Insert Figure 1

The phase diagrams of the two systems ZnO-SiO_2 and MnO-SiO_2 have been investigated in references [25,26], respectively. The α-Zn_2SiO_4 crystalline phase is stable up to 1430°C, whereas Mn_2SiO_4 begins to fuse at 1250°C. The incorporation of manganese in the zinc silicate matrix then tends to lower the fusion point and as a consequence to lower the sintering temperature. In the present work, the manganese doping level was relatively high ([Mn]/([Mn]+[Zn]) =10%), whereas in most luminescent applications it is of 5% or less. This was chosen on purpose because a higher Mn content increases the risk of inter-particles sintering. In these conditions the evaluation of the various thermal post treatments with respect to sintering was more reliable.

Based on all these considerations, the thermal treatments were performed between 900 and 1200°C.

3.2. FB hydrodynamics at high temperature

For the two activated fluidization techniques, the optimal fluidization conditions obtained at ambient temperature were applied in this study at high temperature, as reported elsewhere [18].

The preliminary step before post treating the Zn_2SiO_4:Mn powders was to analyze the hydrodynamic behaviour of the FB between 900°C and 1200°C, then to measure the resulting axial profile of temperatures inside the FB, for the two processes of activated fluidization tested. The pressure drop curves at decreasing gas flow rate for the two activated FB processes are given in Fig. 2 at different temperatures.

Insert figure 2

First, the existence of a plateau for DP*=1 proves that fluidization was reached for the two activated FB processes whatever the temperature tested. The minimum fluidization velocity U_{mf} decreased as temperature increased. This trend is logical since fluid/particle interactions in such beds are dominated by viscous forces, which decrease if temperature increases because of the concomitant decrease of gas viscosity (U_{mf} is inversely proportional to the gas viscosity according to the viscous term of the Ergun relation) [10]. At 1200°C, it varied from 1.3 cm/s STP (Standard Temperature and Pressure) to 1.7 cm/s in FB with coarse powders. The same variation was observed at 1100°C, from 1.5 cm/s in vibrating FB to 2 cm/s in FB by adding the coarse powders. It is also interesting to know that during these hydrodynamic experiments, elutriation was about 4 % of the initial bed weight when coarse powders were added and 1 % in vibrated conditions. Particle elutriation was identical whatever the temperature. From these criteria, the vibrated fluidization process is therefore more suitable for post treating the Zn_2SiO_4:Mn particles, since it most often leads to lower gas consumption and to lower particle elutriation.

The resulting axial temperature profiles in the FB for the four nominal temperatures are presented in Fig. 3 for the two activated fluidization processes. The data points presented in the figure correspond to the averages of 3 runs. The uncertainty on temperature measurements was of + or - 10°C. The results were identical for both activated processes.

Insert figure 3

These curves show that a uniform temperature (gradients lower than 20°C) was obtained in the FB from the distributor to the top zone of the bed, as a consequence of the satisfactory hydrodynamics of the FB previously mentioned.

The FB hydrodynamics and thermal characteristics involved in the two activated processes tested therefore appear as suitable for the heat treatment of the micrometric Zn_2SiO_4:Mn powders.

3.3. Comparison of the powders before and after heat treatments

3.3.1. Powder size distribution and morphology

The particles volume median diameter of the as sprayed particles measured by laser light scattering was 2.2 ± 0.1 μm. The volume median diameters of particles after post treatment with the various processes are given in Table 1.

Insert Table 1

The results show that the mean particle diameters remained lower than 2 µm after thermal treatment at 900°C by all the techniques studied. The particles were on average weakly but significantly smaller than the untreated powders: this traduces the intra-particular densification during the solid state reactions and phase transformations occurring up to 900°C.

For FB treated powders, there was still a unique distribution with median diameters lower than 2 µm after treatment at 1000 and 1100°C. The comparison of the two experiments performed at 1100°C in the vibrated HTFBR demonstrates the reproducibility of results provided by this process.

However, in crucible, the median diameter rapidly increased with temperature to reach the millimeter range from 1100 °C. Fig. 4 presents the size distributions of particles before and after treatment at 1100°C in crucible and in the two FB processes. Two populations of particles were observed in crucible at 1100°C, one minor around 10 µm and the most important one near 1 mm. Massive interparticles sintering phenomena occurred then in crucible from 1100°C.

Noticeable inter-particles sintering was observed in vibrated FB at 1200°C (0.1 mm aggregates). At this temperature, the sintering phenomenon was much less significant in the FB activated by adding easy-to-fluidize particles (median volume diameter 5 µm). It should be noted that all samples post-treated by FB activated with coarse powders were sieved prior to analysis in order to remove the coarse particles. A sieve of 80 µm mesh was used to separate the mixtures. However some comparisons of granulometry analyses before and after sieving have been performed showing that no agglomerate of phosphor powders was formed during thermal treatment, even at 1200°C.

Insert figure 4

On Fig. 5 are shown the FEG SEM micrographs of the particles before and after heat treatment at 1100°C by the various processes. The as-synthesized particles (Fig. 5a) were micrometric spheres made of smaller sub-particles. The matter was uniformly dispersed in each micrometric sphere. For the powders post treated in crucible (Fig. 5b), sintering is clearly visible since numerous inter-particles bridges occurred, resulting in the big agglomerates already detected by laser light scattering analysis. Powders treated by activated FB (Fig. 5c and d) were made of isolated micrometric spheres in which smaller sub-particles were observed. The various chemical processes resulted in a densification of the individual sub-particles inside a grain and consequently in the formation of voids. This macro porosity was distributed homogeneously in the spherical grains.

Insert figure 5

3.3.2. Crystallinity

The XRD patterns of $Zn_{1.8}Mn_{0.2}SiO_4$ after post heat treatment at 900°C by the various processes exhibited only the willemite (α) phase. After treatments at higher temperatures up to 1200°C, no more phase transformation was observed but the average crystal size of the α phase increased; this was evidenced by the narrowing of the XRD peaks as illustrated in Fig. 6 for the vibrated FB treated powders. The same behaviour was observed for the powders heated in crucible or in the HTFBR activated by coarse powders.

Insert figure 6

The Scherrer average crystal size was estimated by the Halder, Schoenig and Wanger method [20]. For each diffraction pattern, the six most intense diffraction peaks were analysed and the average value of the crystal size determined from these six peaks was considered for comparison between the samples. These values are given in Fig. 7. In all cases, the average crystal size increased with temperature. Weak differences were observed for the two highest temperatures of treatment: activating the fluidization by adding coarse particles seemed to slightly slow down the crystal growth.

Insert figure 7

3.3.3. Photoluminescence

The Mn^{2+} emission and excitation spectra observed for two representative samples (FB with coarse particles at 1100 and 1200°C) are shown in Fig. 8. The green luminescence from Mn^{2+} in α-Zn_2SiO_4 appears as a relatively broad band pointing at 525 nm, easily recognizable. On the excitation side was seen a broad band in the near UV, this one is assigned to the oxygen to manganese charge transfer state (CTS). Much weaker narrow lines in the visible region are assigned to intra-configurational transitions [27].

The as-sprayed Zn_2SiO_4:Mn^{2+} at [Mn]/([Mn]+[Zn])=10% was a brown powder which exhibited no luminescence. Whatever the process, the powders post-treated at 900°C consisted of the pure willemite phase α-$Zn_{1.8}Mn_{0.2}SiO_4$ from XRD. All exhibited the characteristic green luminescence. Heat treatments at higher temperatures increased the luminescence efficiency. As shown in Fig. 8 (right), observed under excitation in the CTS, a gain of about 20% in luminescence was observed when the heat treatment was performed at 1200°C compared to 1100°C. In Table 2 are presented the relative photoluminescence efficiencies measured at 525 nm under excitation at 250 nm for different post treated powders and the average Scherrer crystal size of the samples. There was no correlation observed between these two characteristics. Indeed it had been demonstrated that the effect of increasing crystal size on the photoluminescence efficiency of SP phosphors did not prevail when excitation was performed in the CTS [9,28].

Insert figure 8

Insert table 2

For the cases studied, the disappearance of residual absorption with increasing post-treatment temperatures was the major cause of photoluminescence improvement. The diffuse reflectance (DR) spectra of the powders in the near UV and visible wavelength range were recorded as illustrated in Fig. 9. The DR spectrum for the as-synthesized $Zn_{1.8}Mn_{0.2}SiO_4$ (Fig. 9a) exhibited a very low DR% (equivalent to a strong absorption), in the whole wavelength range, which explains the brownish color of the powder, and a well defined step at 380nm in the near UV. As annealing proceeded, the $Zn_{1.8}Mn_{0.2}SiO_4$ powders became whiter and whiter. The DR spectrum of the powder treated at 1100°C (Fig. 9b) exhibited residual absorption between 400 and 800 nm and the step at 380 nm. The heat treatment at higher temperature (1200 °C) resulted in the disappearance of these features from the DR spectrum (Fig. 9c).

The step at 380 nm corresponds to the absorption by ZnO; for comparison, the DR spectrum recorded on nanometric ZnO powders elaborated by SP [29] is also shown (Fig.

9d). As for the absorption between 400 and 800nm, we assign it to the presence of manganese ions at oxidation degrees higher than 2, since $Mn^{n>2+}$ salts are usually colored. Both effects are detrimental to the luminescence efficiency: residual absorption in the visible range partially absorbs the green emission and absorption in the near UV by ZnO competes with that of the willemite phase but does not produce the green emission.

After heat treatment at 1200°C, the DR spectrum exhibited only absorption by the willemite phase α-$Zn_{1.8}Mn_{0.2}SiO_4$, and the photoluminescence was maximum.

As indicated in table 2, annealing in FB activated with coarse powders at 1100°C enhanced the luminescence more than the two other methods at the same temperature. Annealing at 1200°C in FB activated with coarse powders and in crucible gave similar luminescence intensities.

Insert figure 9

4. Conclusion

Micrometric manganese doped zinc silicate $Zn_2SiO_4:Mn^{2+}$ powders with a molar doping level of 10% in Mn were synthesized by spray pyrolysis at 550°C and then post treated at ambient air pressure between 900 and 1200°C, in order to crystallize the willemite phase and to get intense luminescence properties. Three heat treatment processes were studied: (i) a conventional static bed process in a crucible, (ii) a fluidization process activated by adding coarse powders, (iii) another fluidization process activated by column vibrations.

The activation of fluidization was necessary because of the high interparticle forces existing in such cohesive powders. The choice of the methods of activation was based on previous results obtained at ambient temperature. Convenient fluidization conditions were obtained for the two processes of activated fluidization, leading to isothermal beds at high temperatures.

The size distribution by laser light scattering analysis, the crystallinity by X-ray diffraction, the morphology by scanning electron microscopy and the luminescence intensity of particles before and after thermal treatments, were analysed and compared for the three processes tested. Sintering started to occur at 1000°C in crucible whereas it was detected only at 1200°C in the fluidization processes. During annealing up to 1100°C by each of the two activated fluidized bed processes, the initial morphology of the powder was preserved. Unconnected micrometric spheres made of interconnecting dense sub-particles and voids were observed by electron microscopy. Vibrated fluidization appeared to be slightly less efficient in limiting sintering phenomena than fluidization activated by coarse particles. However, it most often led to lower gas consumption and lower elutriation than fluidization activated by adding coarse powders. Another drawback for the latter process is that it needed an additional separation step after treatment.

Only the willemite α crystalline phase was detected by XRD in samples treated at 900°C and above by the three processes. The average Scherrer crystal size increased with temperature for the conditions tested from 40 to 80 nm. The photoluminescence observed for all powders post-treated at 900°C and above was the well known emission of the manganese-doped willemite green phosphor. The samples treated at the highest temperature exhibited the highest efficiency. However, no direct correlation was established between the green emission intensity under near UV excitation and the crystal size. On the other side, the examination of the diffuse reflectance spectra put forward that residual ZnO and manganese ions at oxidation state higher than 2 were still present in samples post heated at 1100°C. Both

residues disappeared at the highest temperature tested (1200°C), which resulted in greater luminescence efficiency.

Annealing at 1200°C in fluidized bed activated with coarse particles appeared to be the best process since maximal luminescence efficiency was reached for minimal sintering.

The synthesis of $ZnSiO_4$:Mn powders by spray pyrolysis followed by post treatment at high temperature in activated fluidized bed proves then to be a valuable solution for the production of green phosphor powders of micrometric size and spherical shape. More generally, these results open promotional perspectives to post treat (i.e. crystallize, reduce, graft or even coat by chemical vapour deposition), micrometric powders in reproducible and uniform conditions in an easy-to-scale-up technology, the fluidization process.

Acknowledgements

The authors wish to thank Pr. J.P. Couderc for his valuable contribution. This work was supported by the French Ministry of Research (RNMP/POSUMIC) and the french Midi-Pyrénées region.

References

[1] C. Ronda, J. Lumi. 72-74 (1997) 49.
[2] J. Koike, IDW97 (1997) 617.
[3] T. Jüstel, H. Bechtel, H. Nikol, C. Ronda, D. Wiechert, Electrochem. Soc. Proc. 98 (1998) 103.
[4] A. Morell; N.E. Khati, J. Electrochem. Soc. 140 (1993) 2019.
[5] C. Ronda, T. Amrein, J. Lumin. 69 (1996) 245.
[6] M. Ryuichi, N. Kazuhiro, Mater. Res. Bull. 29 (1994) 751.
[7] I. Lengorro, F. Iskandar, H. Mizushima, B. Xia, K. Okuyama, N. Kijima, Jap. J. Appl. Phys. 39 (2000) L1051.
[8] Y.C. Kang H.D. Park, Appl. Phys. A. 77 (2003) 529.
[9] N. Joffin, B. Caillier, J. Dexpert-Ghys, M. Verelst, G. Baret, A. Garcia, B. Guillot , J. Galy, R. Mauricot, S. Schamm, J. Phys. D: Appl. Phys. 38 (2005) 3261.
[10] D. Kunii, O. Levenspiel, Fluidization Engineering, second edition, John Wiley & sons Inc., New York, 1991, pp. 77-83.
[11] D. Geldart, Types of gas fluidization, Pow. Technol. 7 (1973) 285.
[12] J. Visser, Pow.Technol., 58 (1989) 1.
[13] J. Kim, G.Y. Han, Pow. Technol. 166 (2006) 113.
[14] C. Zhu, G. Liu, Q. Yu, R. Pfeffer, R.N. Dave, C.H. Nam, Pow. Technol. 141 (2004) 119.
[15] Y. Liu, S. Kimura, Pow. Technol. 106 (1999) 160.
[16] C. Xu, J. Zhu, Pow. Technol. 161 (2006) 135.
[17] N. Joffin, PhD thesis, Institut National Polytechnique, Toulouse, France, 2004.
[18] S. Alavi, B. Caussat, Pow. Technol. 157 (2005) 114.
[19] S. Alavi, N. Joffin, M. Vérelst, B. Caussat, Chem. Eng. J. 125 (2006) 25.
[20] B. Warren, X ray Diffraction, Dover publication Inc., New York, 1990.
[21] H. Rooksby, A. MacKeag, Trans. Farad. Soc. 37 (1941) 308.
[22] Y. Kang S. Park, Mat. Res. Bull. 35 (2000) 1143.
[23] S. Kai, T. Don, J. Am. Chem. Soc. 118 (1996) 3459.
[24] J. Lin, D. Sanger, M. Menning, K. Barner, Mater. Sci. Eng. B 64 (1999) 73.
[25] E. Bunting, Bur. Stand. J. Res. 4 (1930) 134.
[26] F. Glasser, Amer. J. Sci. 256 (1958) 405.
[27] G. Blasse, B. Grabmeier, Luminescent Materials, Springer-Verlag, Berlin, 1994.
[28] N. Joffin, J. Dexpert-Ghys, M. Vérelst, G. Baret, A. Garcia, J. Lumin. 113 (2005) 249.

[29] C. Rossignol, M. Vérelst, J. Dexpert-Ghys, S. Rul, Advances in Science and Technology 45 (2006) 237.

Figure captions

Figure 1: High temperature XRD patterns of Zn_2SiO_4 prepared by SP at 500°C. a): as-sprayed powder analysed at room temperature; b): observation at 750°C; c): observation at 900°C. Peaks noted "Pt" come from the platinum sample holder

Figure 2: Evolution of the dimensionless pressure drop DP* versus decreasing air velocity in (a) the vibrated FB and (b) the FB activated with coarse powders

Figure 3: Axial temperature profile along the FB reactor for the four nominal temperatures

Figure 4: Particle volume diameter distribution of powders before and after thermal treatment at 1100°C

Figure 5: FEG SEM views of the Zn_2SiO_4:Mn^{2+} powders (a) before and after treatment at 1100°C (b) in crucible, (c) in FB with coarse particles and (d) in vibrated FB

Figure 6: XRD patterns of $Zn_{1.8}Mn_{0.2}SiO_4$ powders before and after treatments in vibrated fluidized bed at the various temperatures tested. Left side: full range analysed (10° to 80° in 2θ). Right side: detail of the 46° to 50° range illustrating the peak narrowing at higher temperature

Figure 7: Variation of the Scherrer crystal size with annealing temperature for the different post treatment techniques

Figure 8: Luminescence spectra of $Zn_{1.8}Mn_{0.2}SiO_4$ samples treated in fluidized bed activated by coarse particles at 1100°C (thin) and at 1200°C (thick). Left: excitation spectra (emission at 525nm). Right: emission spectra (excitation at 250nm)

Figure 9: Diffuse reflectance spectra measured on a) as-synthesized $Zn_{1.8}Mn_{0.2}SiO_4$; b) and c) samples treated in fluidized bed activated by coarse particles at 1100°C and 1200°C respectively; d) ZnO synthesized by spray pyrolysis

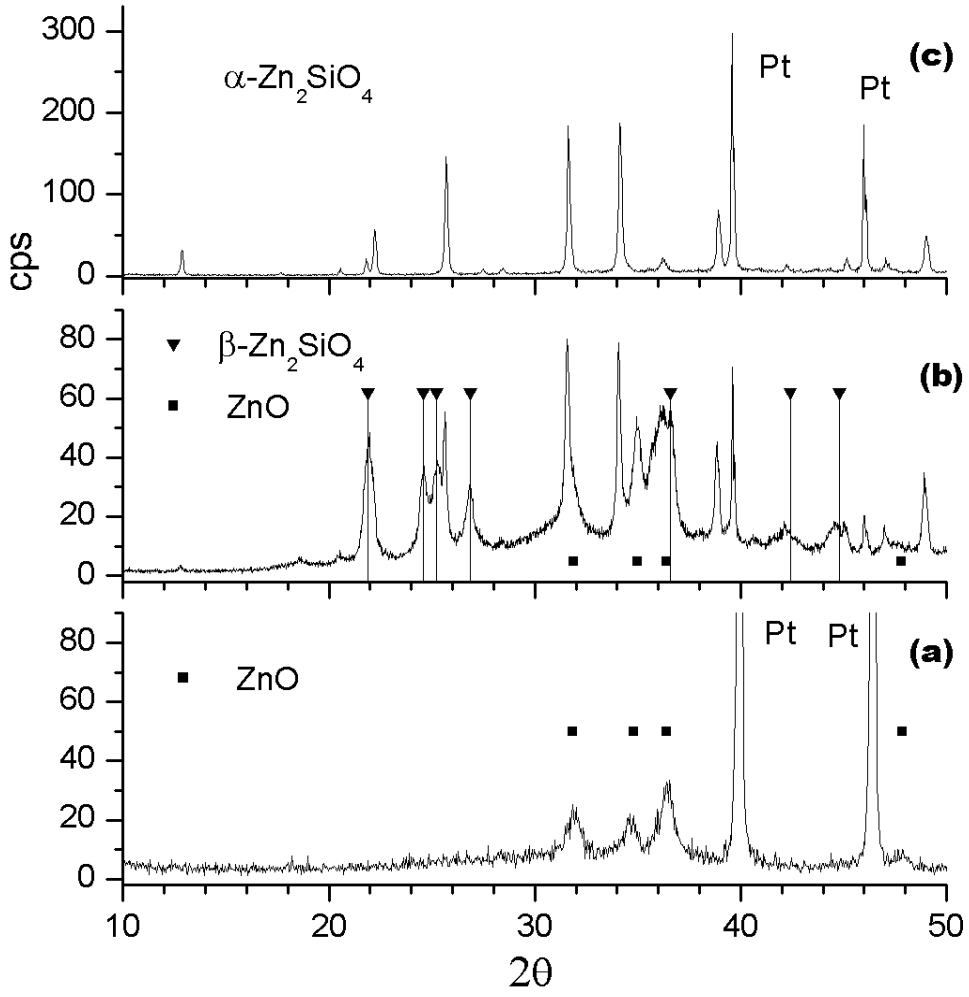
300
200
100
0
cps
α-Zn2SiO4
Pt
Pt
(c)
80
60
40
20
0
β-Zn2SiO4
ZnO
(b)
80
60
40
20
0
ZnO
Pt
Pt
(a)
10
20
30
40
50
2θ

Figure 1

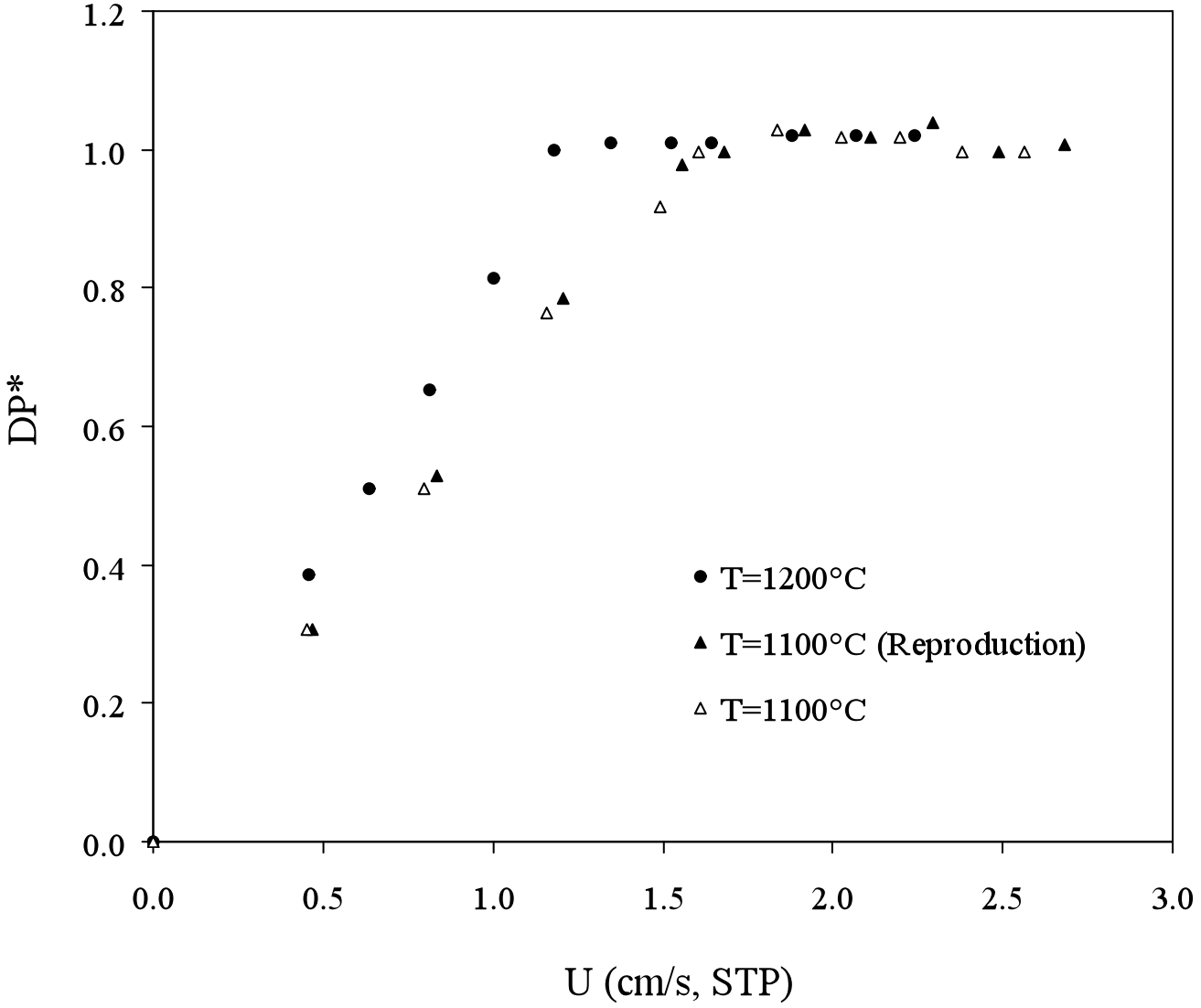
1.2
1.0
0.8
0.6
0.4
0.2
0.0
DP*
0.0
0.5
1.0
1.5
2.0
2.5
3.0
U (cm/s, STP)
T=1200°C
T=1100°C (Reproduction)
T=1100°C

(a)

Figure 2(a)

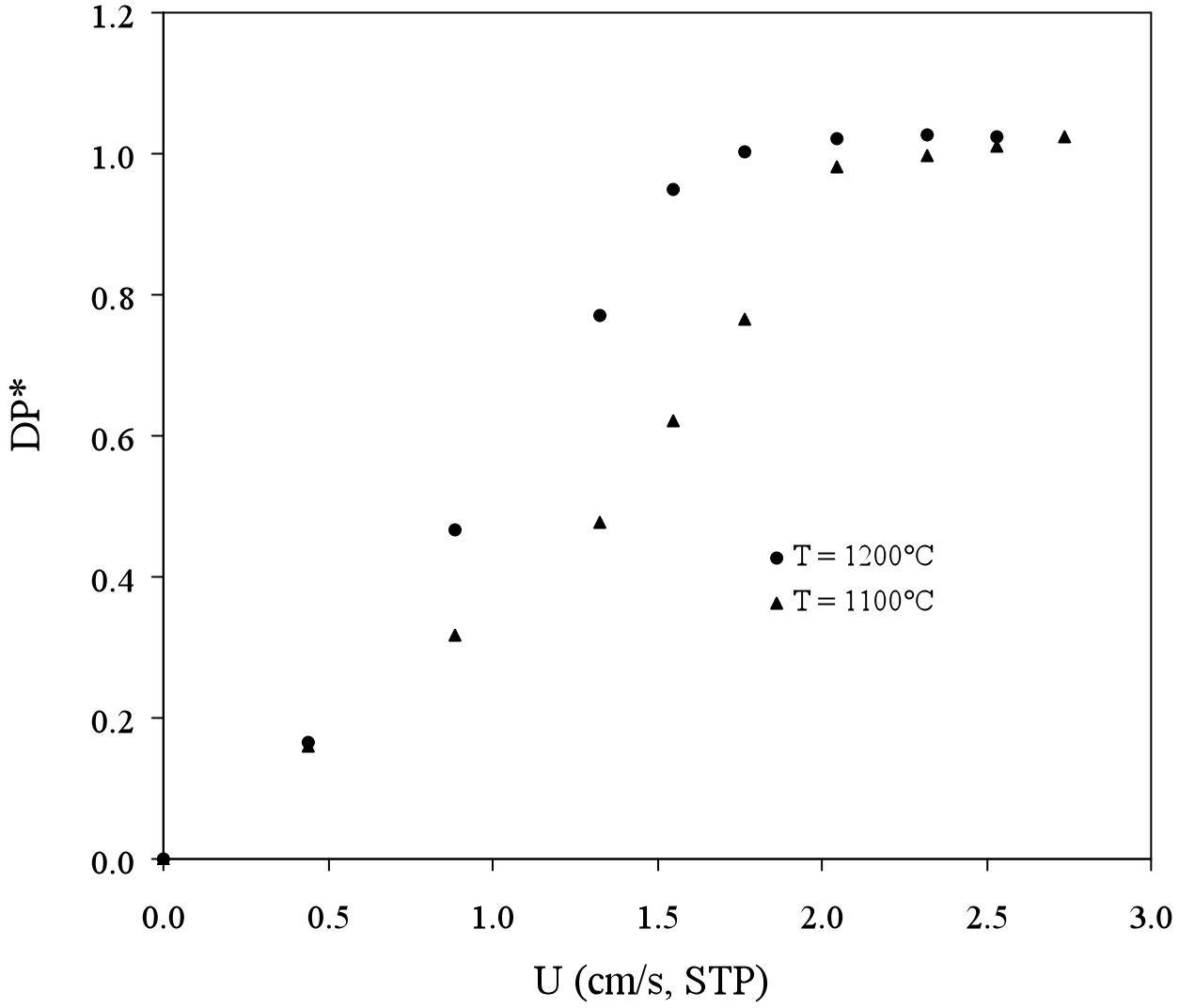

(b)

Figure 2(b)

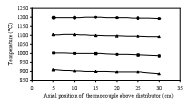
Temperature (°C)
Axial position of thermocouple above distributor (cm)

Figure 3

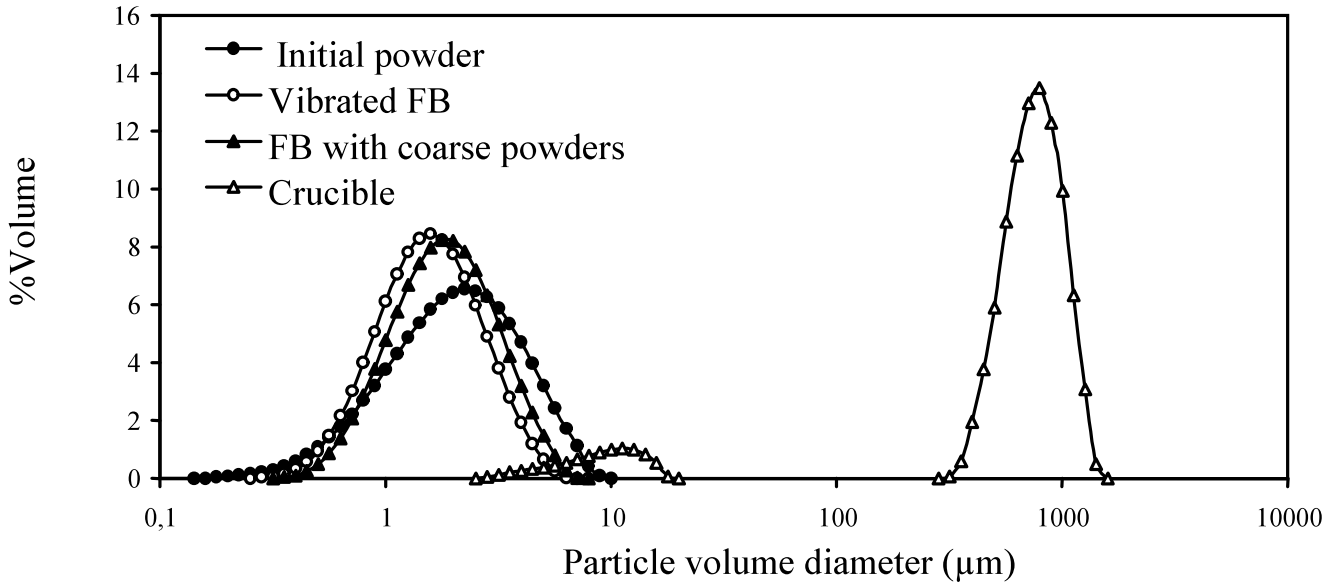
16
14
12
10
8
6
4
2
0
%Volume
Initial powder
Vibrated FB
FB with coarse powders
Crucible
0,1
1
10
100
1000
10000
Particle volume diameter (µm)

Figure 4

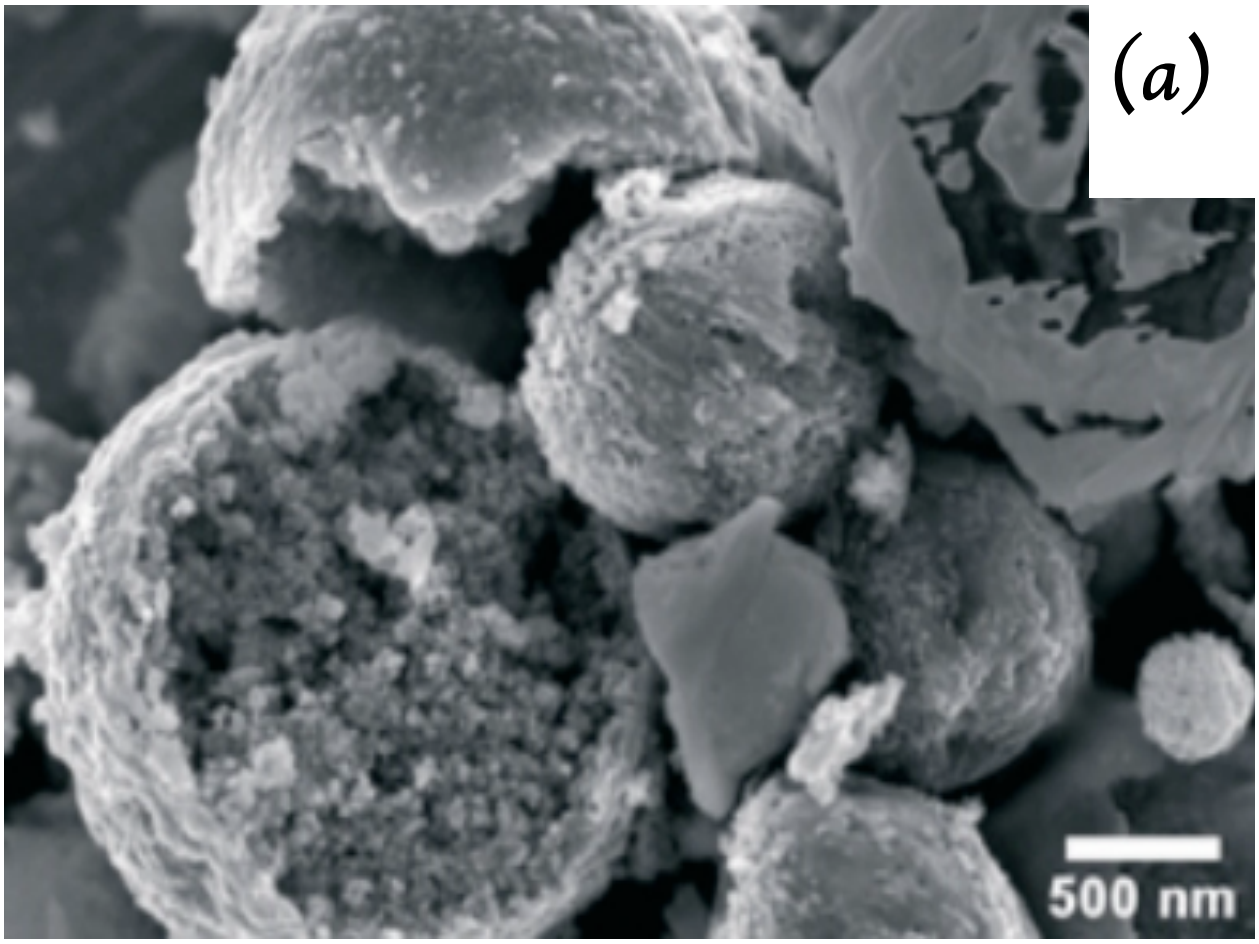

Figure 5(a)

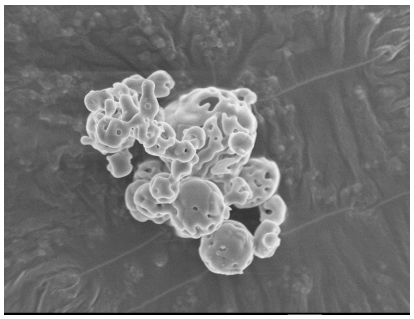

(b)

Figure 5(b)

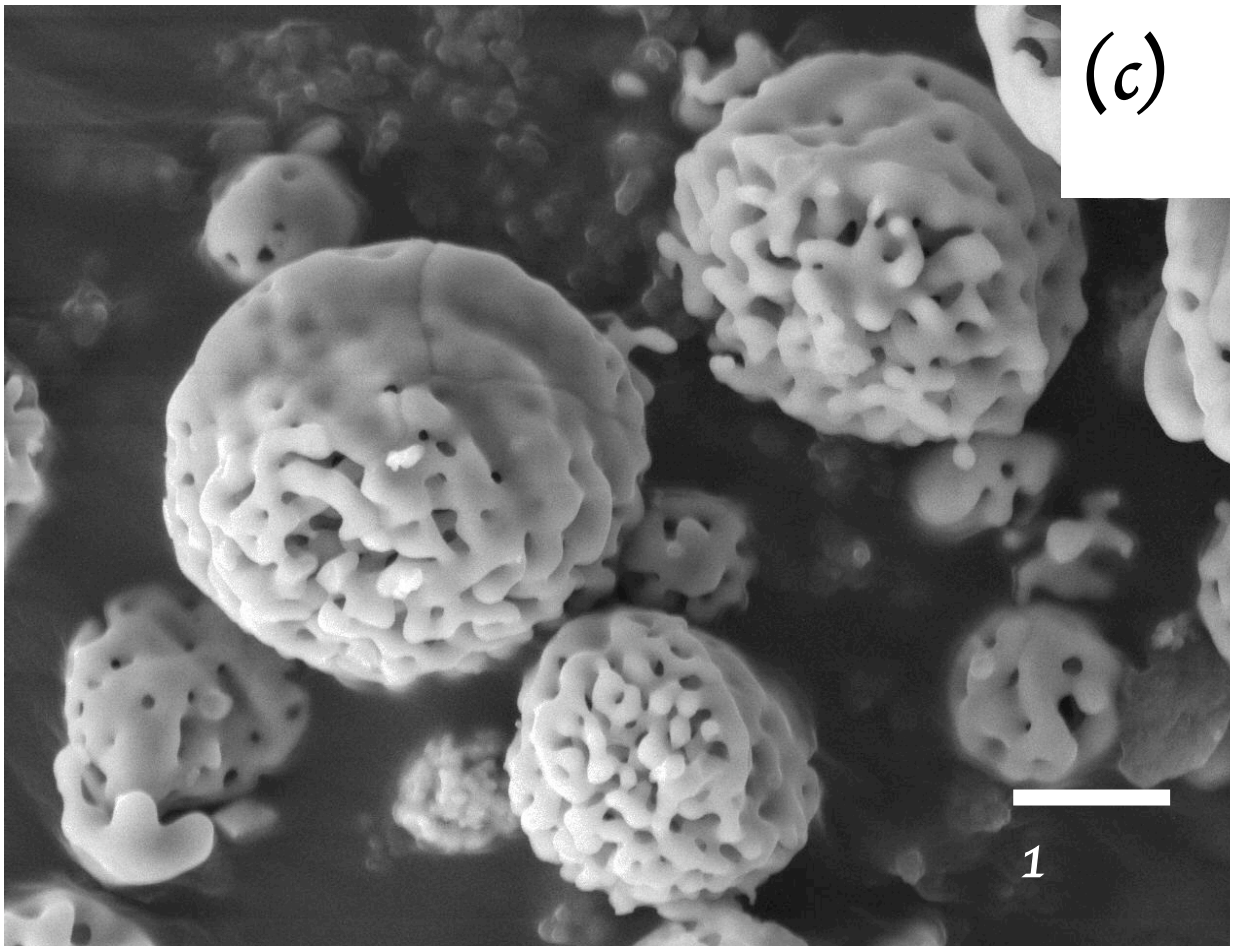

Figure 5(c)

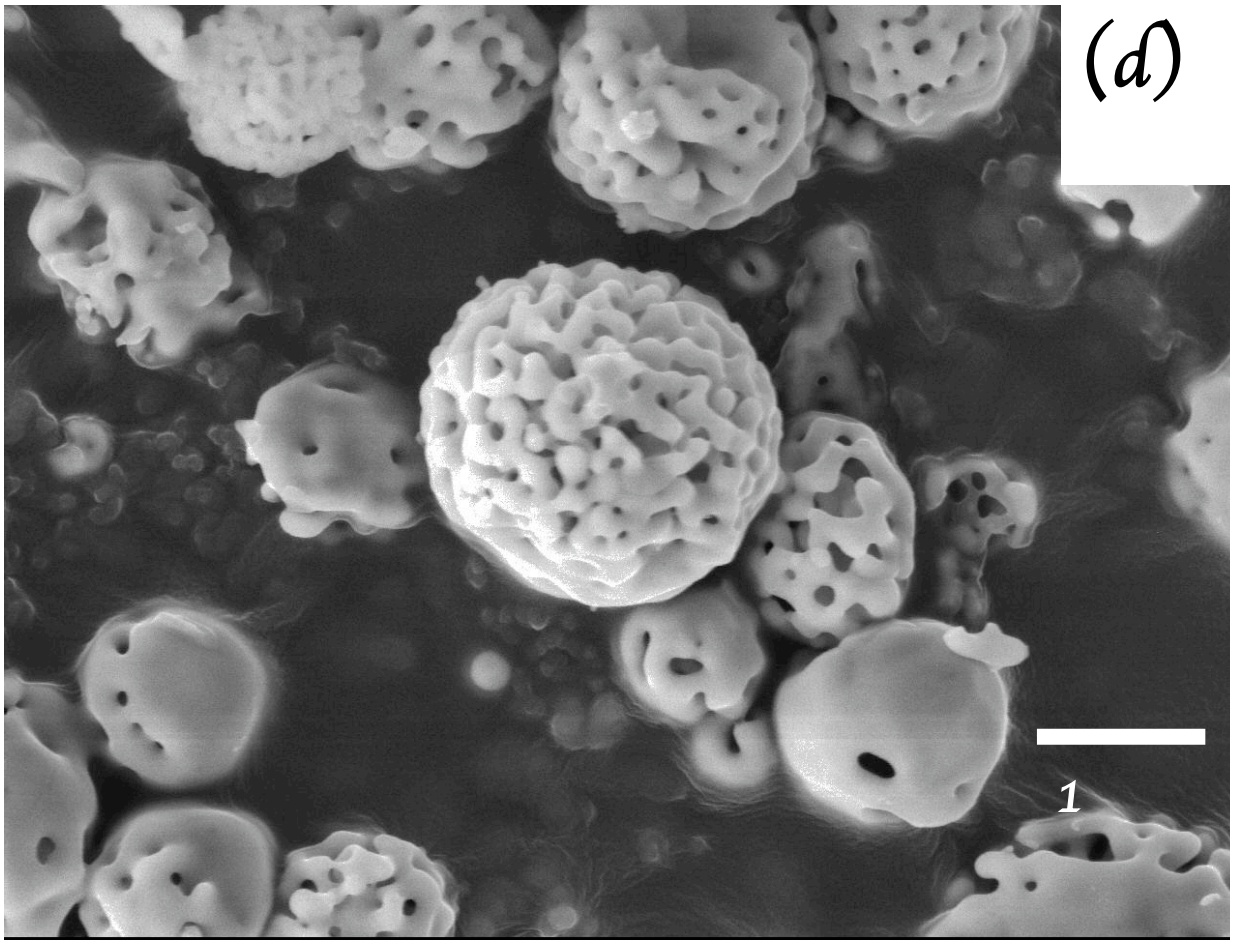

Figure 5(d)

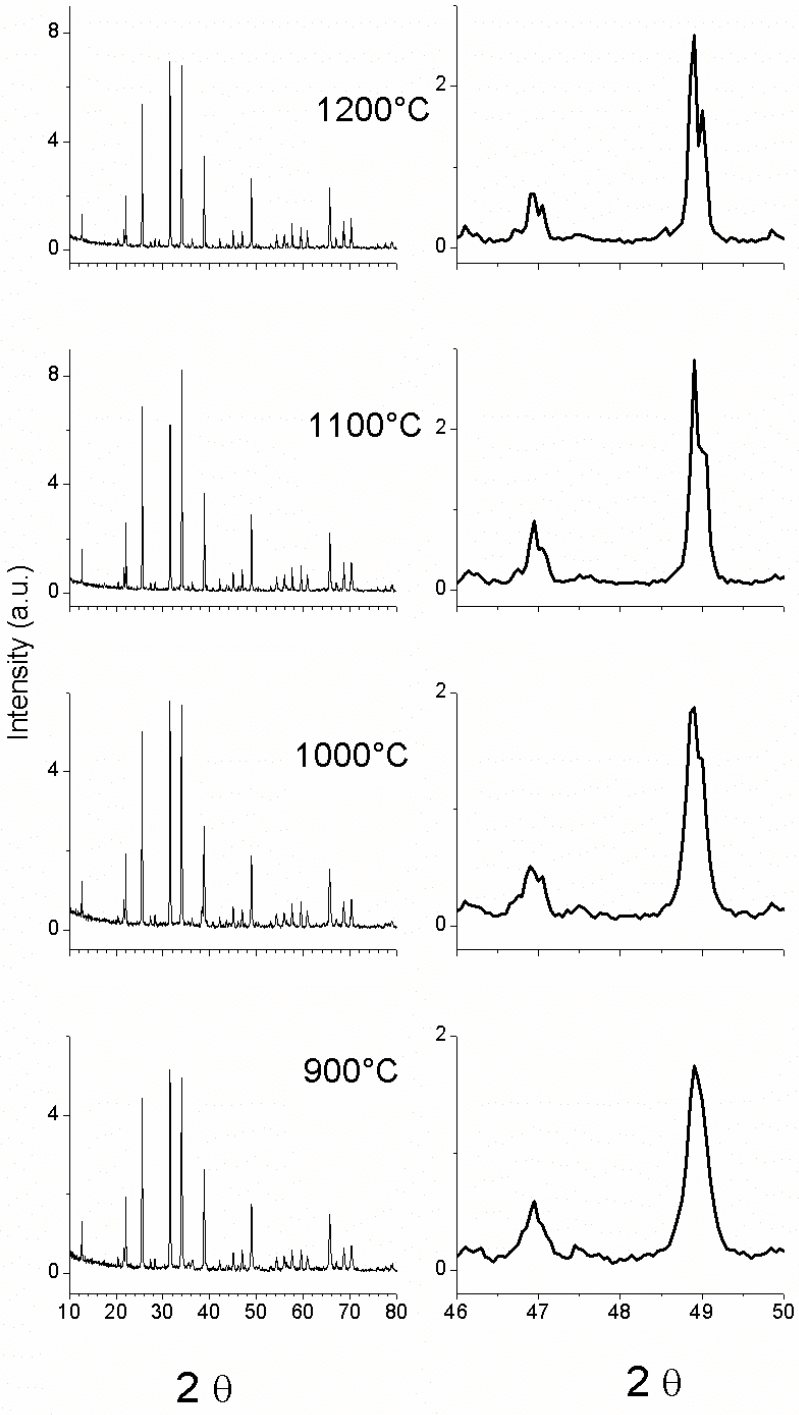

Figure 6

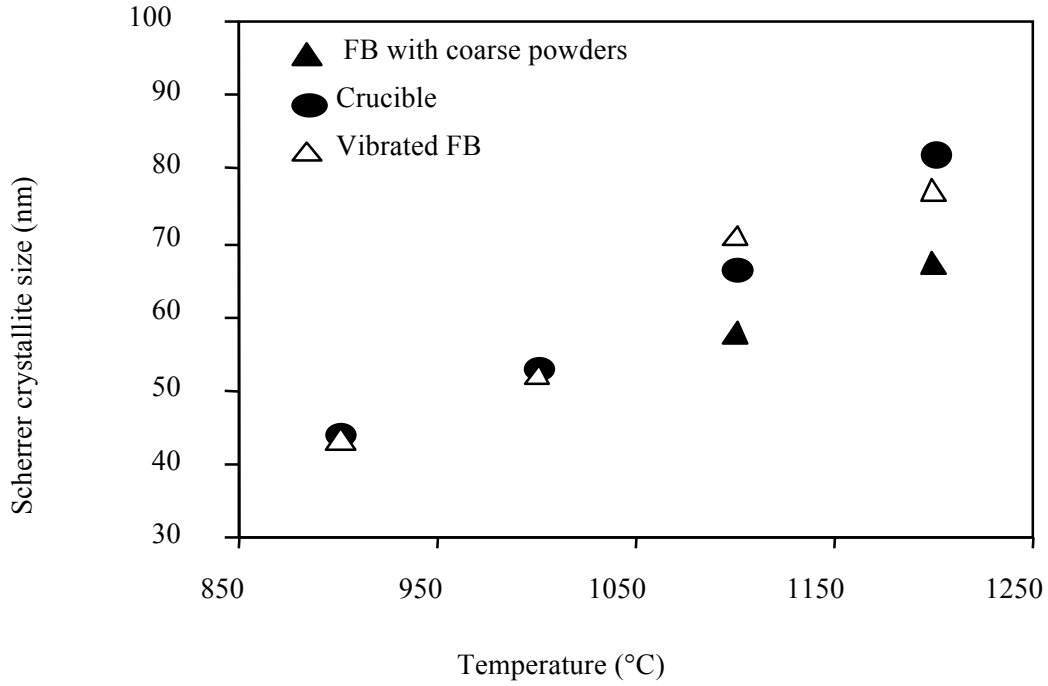
100
90
80
70
60
50
40
30
Scherrer crystallite size (nm)
FB with coarse powders
Crucible
Vibrated FB
850
950
1050
1150
1250
Temperature (°C)

Figure 7

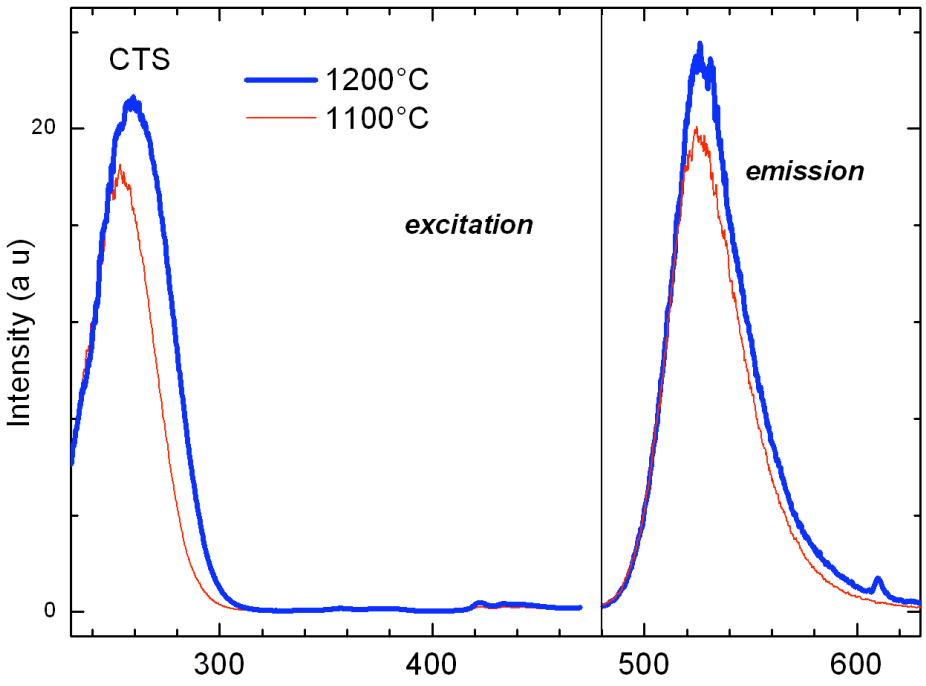
CTS
1200°C
1100°C
excitation
emission
Intensity (a u)
20
0
300
400
500
600

Figure 8

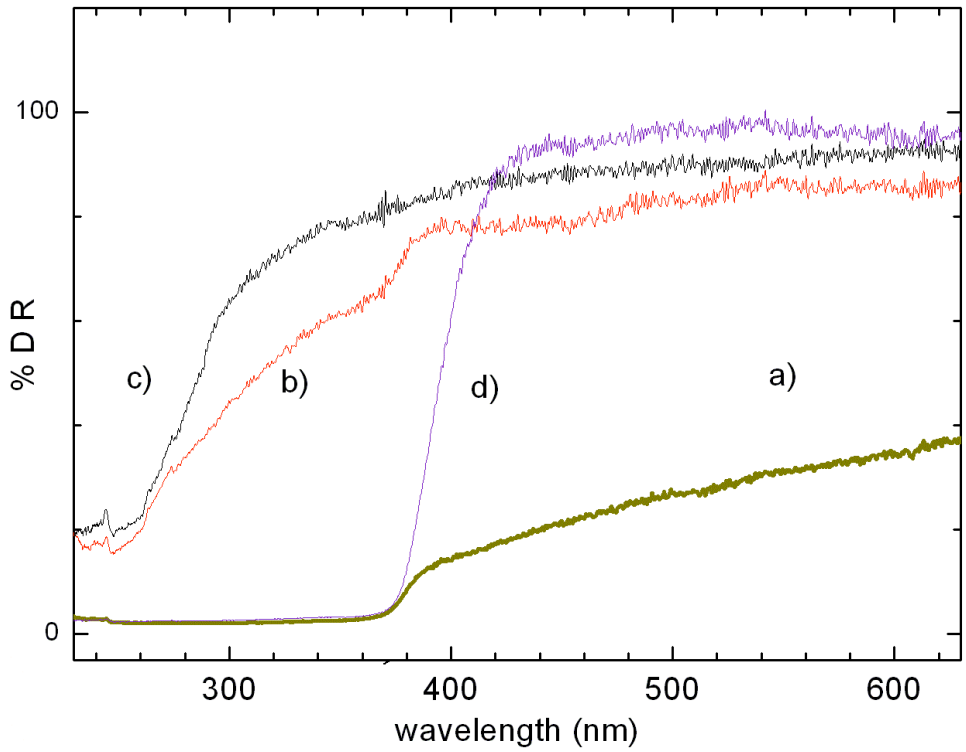

Figure 9

Table 1: Volume median diameter of powders before and after annealing by the various techniques

Temperature	Crucible	Vibrated FB	FB with coarse particles
900 °C	1.5 ± 0.1 µm	1.9 ± 0.1 µm	-
1000 °C	14.2 ± 0.7 µm	2.1± 0.1 µm	-
1100 °C	767 ± 35 µm	1.7 ± 0.1 µm	1.9± 0.1 µm
1100 °C (reproducibility)	-	1.8 ± 0.1 µm	-
1200 °C	1088 ± 50 µm	80.5 ± 4 µm	5.2 ± 0.2 µm

Table 2: Luminescence relative intensity (excitation at 250 nm, emission at 525 nm) versus average crystal size (from Fig. 7)

Heat Treatment technique	FB with coarse powders		Vibrated FB	Crucible	
Annealing temperature (°C)	1100	1200	1100	1100	1200
Scherrer crystal size (nm)	58 ± 3	65 ± 3	70 ± 4	67 ± 3	82 ± 4
Luminescence intensity (%)	86 ± 5	100 ± 5	79 ± 4	80 ± 4	98 ± 5